forests

MDPI

Article

Effect of Supercritical CO_2 Drying on Moisture Transfer and Wood Property of *Eucalyptus urophydis*

Lin Yang [1,2,3] and Honghai Liu [1,2,*]

[1] College of Furnishings and Industrial Design, Nanjing Forestry University, Nanjing 210037, China; yanglin@njfu.edu.cn

[2] Co-Innovation Center of Efficient Processing and Utilization of Forest Resources, Nanjing Forestry University, Nanjing 210037, China

[3] Key Laboratory of Bio-Based Material Science & Technology (Northeast Forestry University), Ministry of Education, Harbin 150040, China

* Correspondence: liuhonghai2020@njfu.edu.cn

Received: 14 September 2020; Accepted: 16 October 2020; Published: 20 October 2020

Abstract: Wood dried using supercritical CO_2 has unique properties because water is removed directly from the cell lumens through the cycling between supercritical and gas phases. *Eucalyptus urophydis* green wood was dried by supercritical CO_2 at 50 °C and pressure of 10, 20, and 30 MPa; the effect of supercritical CO_2 drying on moisture content distribution and transfer, as well as the permeability and extractive content of the wood, was investigated. The results showed that the supercritical CO_2 drying rate was high, showing the highest drying rate at 20 MPa and the lowest at 10 MPa. Drying rate increased with pressure below 20 MPa in this study; drying rate represented no positive relation to pressure over 20 Mpa. Moisture content distribution was more uneven in the low-pressure drying conditions and in the middle transverse section of the specimens. The moisture content gradient in tangential was greater than that in longitudinal, especially for the drying of 10 MPa, indicating that water was removed mainly in the former direction of wood. More extractives were removed from wood at higher pressure during supercritical CO_2 drying. Bordered pits were broken up more at higher pressure conditions. The decreased extract yields and increased amount of opened bordered pits increased the permeability of the wood after supercritical CO_2 drying.

Keywords: supercritical carbon dioxide drying; moisture content distribution; moisture transfer; permeability; extractives

1. Introduction

Eucalyptus trees have been planted widely in south China. Although most Eucalyptus species are used for pulping, papermaking, and wood-based panels, certain species have a potential for the production of solid-wood products, such as furniture and flooring, due to their high density and mechanical strength [1]. Thus, recently the wood processing industry has paid more attention to the processing and utilization of eucalyptus wood. However, collapse during conventional kiln drying (CKD) is a severe defect limiting its use as a solid-wood material [2,3].

Normally, shrinkage property is the inherent character of wood. Wood shrinks when its moisture content is lower than its fiber saturation point (FSP), and the wood cells do not deform as the wood shrinks. However, collapse is a severe shrinkage of wood which results in cells severely deforming due to negative water tension in the wood during the early stages of CKD where the wood has a high moisture content (MC) [4–6]. In order to decrease the prevalence of collapse during CKD, some pretreatments can be applied to alleviate the conditions causing collapse, such as pre-steaming or boiling, pre-microwaving, and pre-freezing [7–9]. Other methods, such as improving the humidity

of drying conditions during or after drying, can promote recovery from collapse [10,11]. In addition, some special drying methods, including radio-frequency/vacuum drying, freeze-drying, and supercritical CO_2 drying (SCD), have been applied to eucalyptus wood, and can reduce the extent of the deformation of the wood [12–14], especially SCD.

Supercritical CO_2 ($SuCO_2$) fluid has a lower supercritical temperature (31.1 °C) and supercritical pressure (7.38 MPa) [15]; it has excellent solubility and heat transfer characteristics, and other good properties such as availability, non-toxicity, non-flammability, high recovery rate, and strong process selectivity [16]. These characteristics indicate that $SuCO_2$ can be of great use for various wood-related applications, such as impregnation, extraction, and drying. The SCD method, put forward in patents for the first time, dewaters wood by changing the pressure to circulate CO_2 between the supercritical phase and the gas phase via the pressure difference in the decompression process [17]. $SuCO_2$ fluid was also used to dry radiata pine, and it was found that the wood samples with an initial MC of 174% were successfully reduced to 39% after seven cycles between supercritical fluid and gas phases [18]. This method could prevent wood cracking caused by surface tension and significantly reduce wood collapse resulting from negative water tension [19–21]. Additionally, during SCD, the hydrothermal softening due to lignin heating under saturated conditions could potentially release the built-up stresses, resulting in less collapse [22]. This method can dry wood fast with few drying defects [23] and has a huge potential in the application of drying for refractory eucalyptus wood. Some scholars have explored the characteristics of drying rate, moisture profiles, and wood shrinkages, and the mechanism of moisture removal and $SuCO_2$ diffusion [24–27]. However, few studies were related to the effect of SCD on moisture transfer in wood radial, tangential, and longitudinal directions, and on wood permeability and extractives.

Compared to drying temperature, the effect of drying pressure plays more of a role in water removal during SCD [17,18]; therefore, *Eucalyptus urophydis* wood was dried by SCD at 50 °C and different pressures of 10, 20, and 30 MPa in this study. The main objective was to explore the effect of SCD on moisture transfer, permeability, and extractives of wood.

2. Materials and Methods

2.1. Materials

Green wood of *Eucalyptus urophydis* was obtained from Guangxi, China. The initial MC was about 119% and the basic density was 0.502 g/cm^3. The logs were converted into timber (heartwood) of 25(R) × 30(T) × 1000(L) mm and then were sawn into specimens of 25(R) × 30(T) × 100(L) mm. Thereafter, they were wrapped with plastic film and stored at 4 °C in a refrigerator for later use. In this study, a total of nine specimens of 25(R) ×30(T) ×100(L) mm were random selected and divided into three groups (3 end-matched specimens in each group for each drying condition) for different SCD tests. The specimens were free of knots and other defects (See Figure 1).

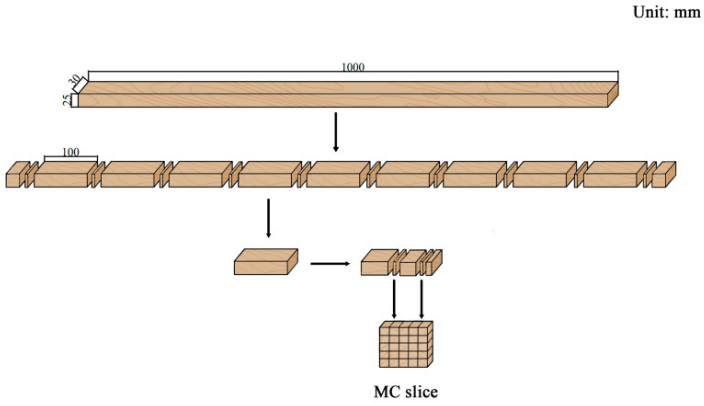

Figure 1. Schematic diagram of drying specimens cutting.

2.2. Equipment

The apparatus used was a $SuCO_2$ drying device (DY221-50-06, Huaan Supercritical Fluid Extraction Co., Ltd., Nantong, Jiangsu, China). It consisted of a CO_2 storage bottle, a 5 L (ϕ100) and a 2 L (ϕ50) drying vessel, a circulating pump, and two drying adsorption vessels, as shown in Figures 2 and 3. The drying vessel could control pressure from 0.1 to 30 MPa, and temperature from 30 to 70 °C. Liquid CO_2 was supplied to the device from the storage bottle and the supercritical pressure was controlled by the circulating pump. The temperature of the drying vessel was regulated by a heated mantle during the drying process.

Other equipment included an electric heating oven (DHG-905386-III, Shanghai Cimo Medical Instrument Co., Ltd., Shanghai, China), a scanning electron microscope (SEM, FEI Quanta 200, Eindhoven, The Netherland), and an electronic balance, with an accuracy of 0.001 g (Sincere Dedication of Science and Technology Innovation Company, Shanghai, China).

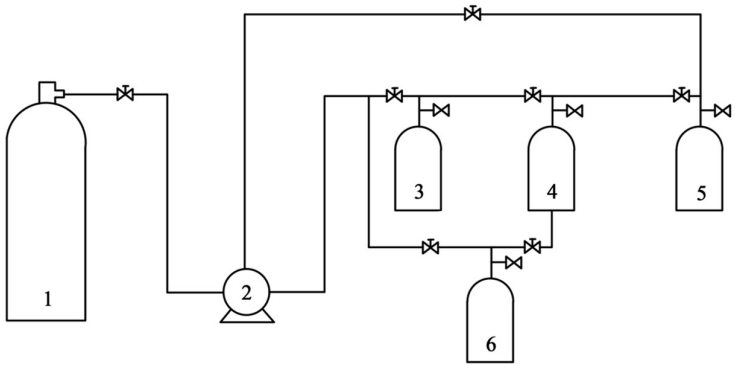

1. CO_2 bottle; 2. Pump; 3, 4. Drying vessel; 5, 6. Drying adsorption vessel

Figure 2. Supercritical CO_2 drying device.

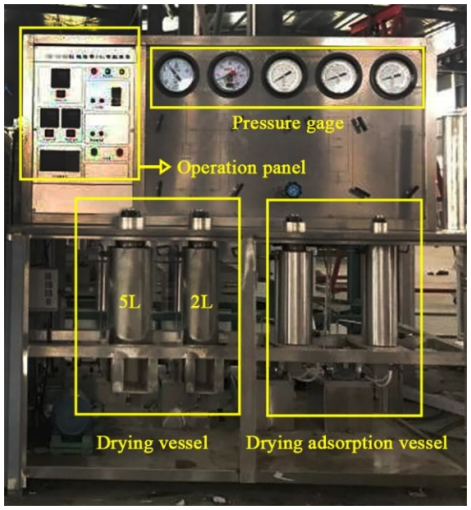

Figure 3. Photo of a part of the supercritical CO_2 drying device.

2.3. Drying Test

All specimens were weighed before each SCD run. For each test, three end-matched specimens were inserted into the drying vessel, and the drying was carried out according to the schedule in Table 1. During the drying process, the specimens were in full contact with $SuCO_2$ at the setting pressure and temperature for a hold time of 60 min. Thereafter, the pressure was decreased to

atmospheric pressure through the escaping of CO_2 gas from the outlet valve. The specimens were taken out from the drying vessel for further sample preparation after cessation of CO_2 emission.

Table 1. Parameters for supercritical CO_2 drying (SCD) process.

Process Parameter	Value
Pressure max (MPa)	10/20/30
Pressure min (MPa)	0.1
Pressurization time (min)	10~30
Hold (min)	60
Decompression (min)	10
CO_2 emission (min)	30
Supercritical temperature (°C)	50

2.4. Determination of Moisture Content and Its Distribution and Drying Rate

The MCs were measured according to GB/T 1931-2009 (National standard of China 2009). MC was determined based on oven-dried weight of specimens. For each test, the specimens were taken out from the drying vessel after decompression, and then were placed into a glass container. Thereafter, two 5 mm thickness slices were sawn from the middle and near one end of a specimen after cessation of CO_2 emission. The slices were dissected into 25 wood blocks (Figure 1), which were then dried at 103 °C to calculate the MC of each block. Thereby, the average MC and distribution in tangential and radial directions in the middle and near one end of a specimen could be evaluated and the drying rate could be determined. The moisture distribution images were drawn by the function of contour using Origin 2020 (OriginLab Corp., Northampton, MA, USA).

2.5. Determination of Extracts of Wood Dried after Supercritical CO_2 Drying

The crushed and processed powder from the wood after SCD was prepared for Soxhlet extraction testing. Three replicates of 2 g each were well wrapped using quantitative filter paper for each drying, and then were extracted using a benzene-ethanol (1:2, v/v) solvent at 60 °C temperature. The extraction duration was 6 h and each cycle was 20 min. The extract yields were calculated using Equation (1).

$$C = (W_1 - W_2)/W_1 \times 100\% \quad (1)$$

where C is the extract yield, W_1 is the mass of absolute dry sample prior to extraction, and W_2 is the mass of wood residue after extraction.

2.6. Microstructure Characterization of Wood after SCD

In order to observe the effect of SCD on the microstructure of the wood, specimens with dimensions of 5(R) × 5(T) × 5(L) mm were prepared after each SCD. The specimens were freeze-dried to a constant weight, and then were fixed on conductive adhesives and coated with gold. The radial sections of the specimens were observed by SEM (FEI Quanta 200, Eindhoven, The Netherland).

2.7. Permeability Evaluation of Wood Dried after Supercritical CO_2 Drying

Wood permeability is a physical property that describes the fluid penetration in wood and is used as an indicator to reflect the degree of wood processing and utilization [28]. To explore the permeability change, the method of measuring water absorption ratios from a previous study was used [29]. In the current study, the water absorption test of the wood was carried out after SCD, and the permeability of the wood was evaluated by water absorption ratio. A total of 5 specimens of 25(R) × 30(T) × 5(L) mm were produced from the left part of the specimens in each drying. Before immersion in water, the specimens were oven-dried at 103 °C to a constant weight and then weighted. Afterwards, the specimens were put into a vessel filled with distilled water, and plastic meshes and stainless-steel ingots were used to ensure that all specimens could absorb water. The water was

replaced once each day during the test. The specimens were taken out of the water in different intervals, and then weighted after wiping the water on the wood surface. The intervals of weight measurement were short in the first day and after that became long. The water absorption ratio was calculated according to Equation (2).

$$W = (W_1 - W_0)/W_0 \times 100\% \quad (2)$$

where W_1 is the mass of specimens after water soaking at different moments and W_0 is the mass of specimens after oven-drying.

3. Results and Discussion

3.1. Characteristics of Drying Rate

The initial and final MCs as well as the drying rate of the three SCD groups and the CKD (Control) group are presented in Figure 4. The drying rate of CKD was obtained from a previous study [23]. The dimensions of specimens for CKD was the same as that of the SCD specimens in this study. The drying conditions of CKD are 50 °C dry-bulb temperature and 84% relative humidity, and the drying time is 1 hour. For SCD, the declined MC of the specimens was from 30 to 50% after 1 h of drying, showing the highest drying rate at 20 MPa and lowest drying rate at 10 MPa. For CKD, the declined MC of specimens was only 5.5% after 1 h of drying. The ratio of drying rate of SCD to CKD is 5.5 to 9.1, indicating that the drying rate of SCD is much faster than that of CKD. From this point, this method is potentially more economical in the industrial application due to the shortened drying time. A previous study showed that the drying rate is influenced by concentrations of dissolved CO_2 and the permeability of wood [16]. Increased pressure improves the concentration of dissolved CO_2 [30] and wood permeability [31], both of which lead to increased drying rates at higher CO_2 pressure. The more CO_2 dissolved in free water, the greater the volume of gas bubbles generated as the CO_2 pressure is lowered, which expels water from wood more rapidly. The penetration of CO_2 into wood is complicated due to the barriers of cell walls and the tortuous diffusion pathways. Therefore, improved permeability promotes the penetration of CO_2 into wood and also reduces the barriers for water flow from wood. However, the drying rate at 30 MPa was lower than that at 20 MPa, which is consistent with previous results [17], indicating that the effect on drying rate is not positively related for higher pressure.

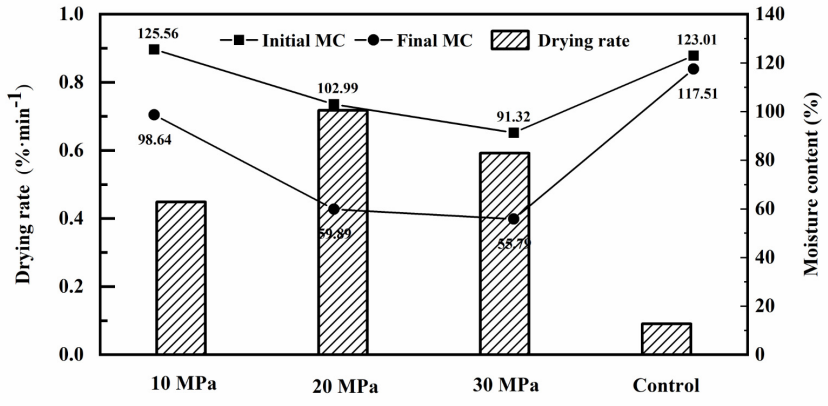

Figure 4. Drying rate and moisture content for 1 h SCD at different pressures.

3.2. Moisture Content Distribution

The 2D images of the MC distribution of specimens after 1 h of SCD at three different pressures are shown in Figure 5. The left and right images represent the MC distribution of locations in the middle and near one end of the specimen, respectively. The average MC in the three left images was higher and the MC distributions were more uneven compared with those in the right images. For all

the images, the interior locations presented higher MCs compared with those near surfaces. These findings show that water in wood is expelled from wood in complicated paths including transverse directions and longitudinal directions. The water in locations near the wood surfaces and the ends of the specimens was easier to be expelled by the generated bubbles of CO_2. However, water in the interior locations in the middle of the specimens was more difficult to be expelled due to the long distance from the interior to the surfaces and ends of the specimens. It can also be seen that the MC distribution of specimens after 1 h of SCD in 10 MPa is more uneven than that of specimens in 20 and 30 MPa. The reasons may be attributed the initial MCs of specimens and the lower hold pressure. The interior water is more difficult to be removed by the expelling of CO_2 bubbles at lower hold pressures when wood has more moisture, resulting in higher interior MC.

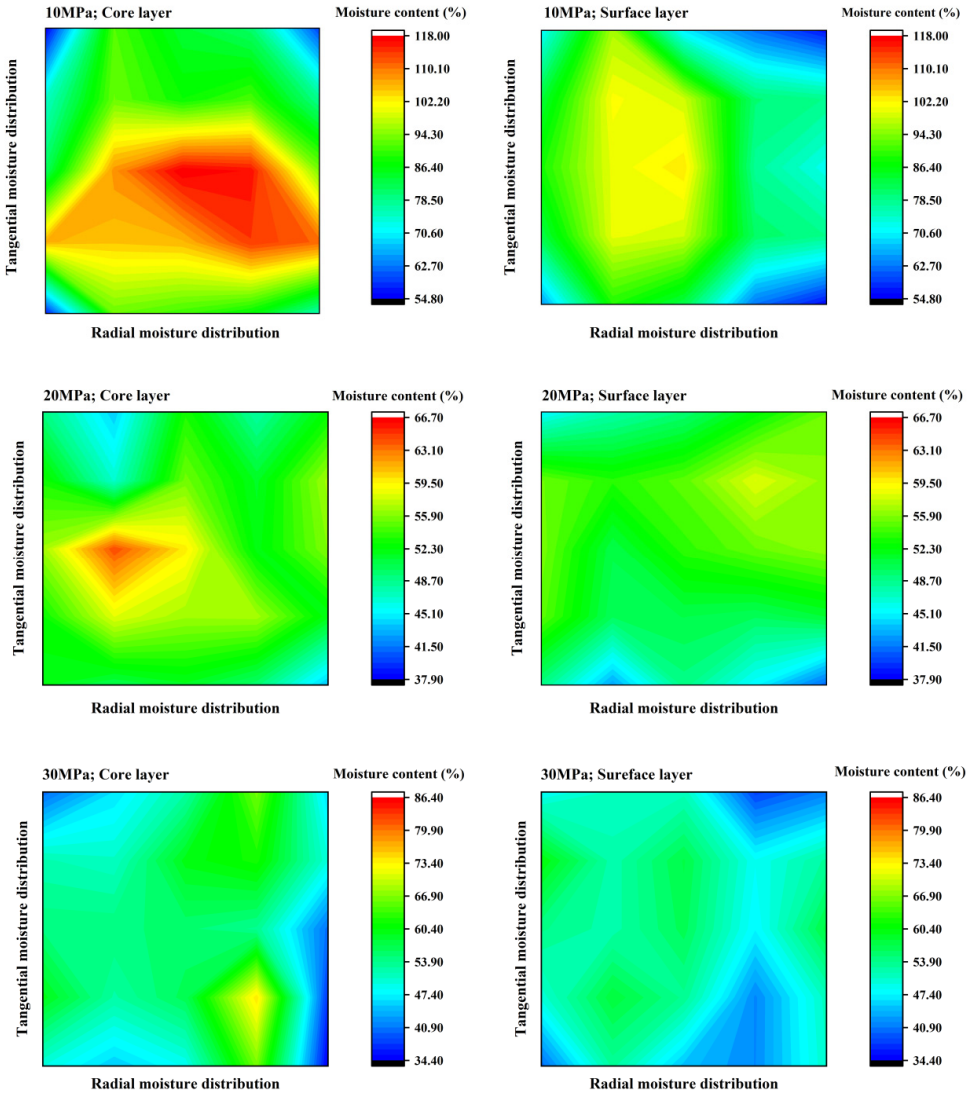

Figure 5. Moisture content distribution of wood after 1 h of SCD at different pressures (core layer: the slice in the middle of a specimen; surface layer: the slice near one end of a specimen).

3.3. Characteristics of Moisture Content Gradient

Moisture content gradient is the difference in moisture content between the inner and outer portions of a board. Figure 6 shows the characteristics of MC gradient in tangential, radial, and longitudinal directions of specimens after 1 h of SCD. The MC gradients in 10 MPa were the biggest,

which was inconsistent with the findings of MC distributions in Figure 5, indicating great differences of MC in longitudinal and transverse sections of wood. The MC gradients of specimens in 20 and 30 MPa decreased significantly compared with those in 10 MPa, leading to relatively small MC differences in wood. For the drying in 10 MPa, there was no difference of MC gradient between the radial and longitudinal directions, but the MC gradient in the tangential direction was almost 2 times those of the radial and longitudinal directions. This implied that free water was removed majorly in the tangential direction from wood in the drying at low hold pressure. For the higher hold pressure of 20 and 30 MPa, although the MC gradients became small in the three directions, the MC gradients in the tangential direction were over 1.5 times that of the longitudinal direction. All these findings show that free water was removed during SCD mainly in the tangential direction; these results are in agreement with previous reports [24,25]. This could be attributed to the more bordered pits existing in the radial walls of wood [32], which control the flow of water between the lumens of adjacent cells. During SCD, the dissolved CO_2 facilitated expulsion as the CO_2 pressure was released and the bubbles of CO_2 gas expanded, which resulted in free water expulsion mainly through tortuous pathways involving cell lumens and the bordered pits that connect those lumens tangentially towards the specimen surfaces. In addition, the higher MC gradient results in a higher drying rate, which could lead to greater negative water tension causing irrevocable damage to the cell wall [33].

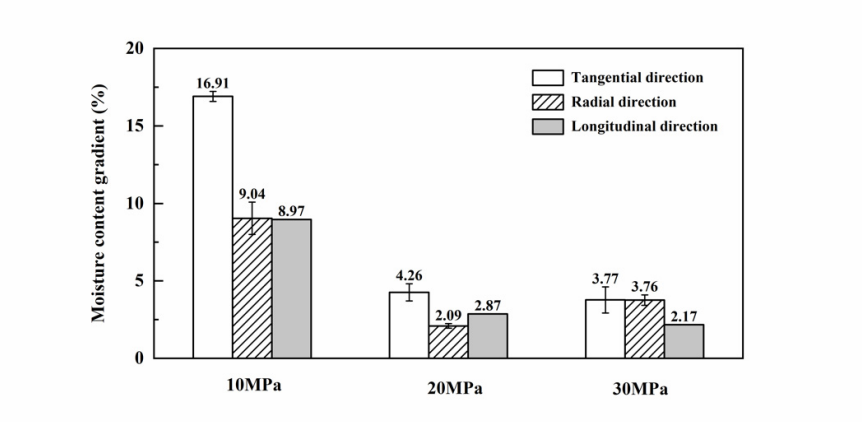

Figure 6. Moisture content gradient of wood after 1 h of SCD at different pressures.

3.4. Extractives of Wood Dried after Supercritical CO_2 Drying

The extract yields of specimens after 1 h of SCD at different pressures are shown in Figure 7. Compared with 10 MPa SCD, the extract yields of wood decreased at 20 and 30 MPa, and there were no obvious differences between wood after 20 and 30 MPa SCD. The main extractives of *Eucalyptus urophydis* obtained using a benzene-ethanol solvent are esters [34], which are more easily dissolved in supercritical CO_2 because of its polarity. The high CO_2 density at high pressure increased its solvent power and therefore, more substances were extracted from the wood as water expulsion [35]. As extractives affect wood permeability, the permeability of specimens could be improved after higher pressure SCD.

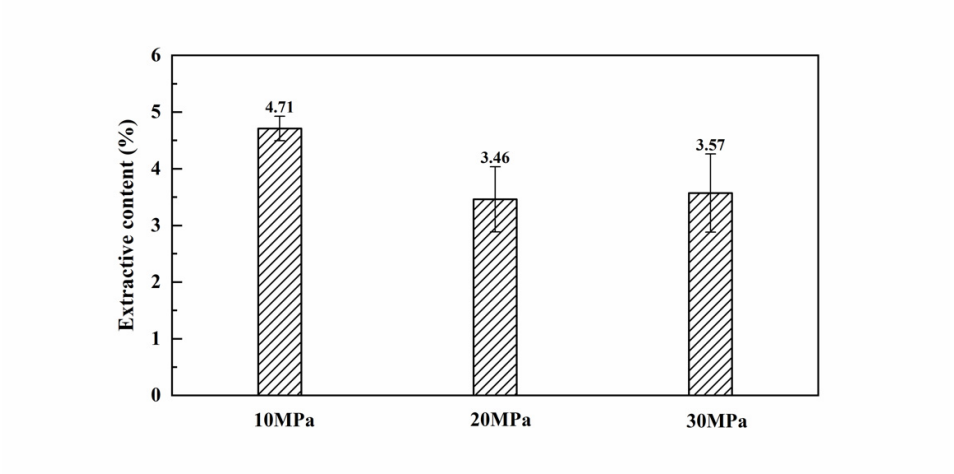

Figure 7. Extract yields of specimens of wood after 1 h of SCD at different pressures.

3.5. Microstructure Characterization of Wood after Supercritical CO_2 Drying

The SEM photographs of specimens after conventional drying (50 °C/60% RH) and SCD are illustrated in Figure 8. The results demonstrate that SCD drying had a remarkable effect on the tissue of cell structures, especially for the higher hold pressure. Few vestured pits opened after conventional dying, while more vestured pits became open after SCD, particularly for the condition of 30 MPa hold pressure. Lots of pits, which are the main moisture transfer passages in the wood interior and control the flow of water between the lumens of cells, were broken up due to the great pressure difference between further locations within wood and locations close to wood surfaces [30,36]. The opened pits improved wood permeability, which benefits supercritical CO_2 diffusing into wood and moisture removal in wood interior.

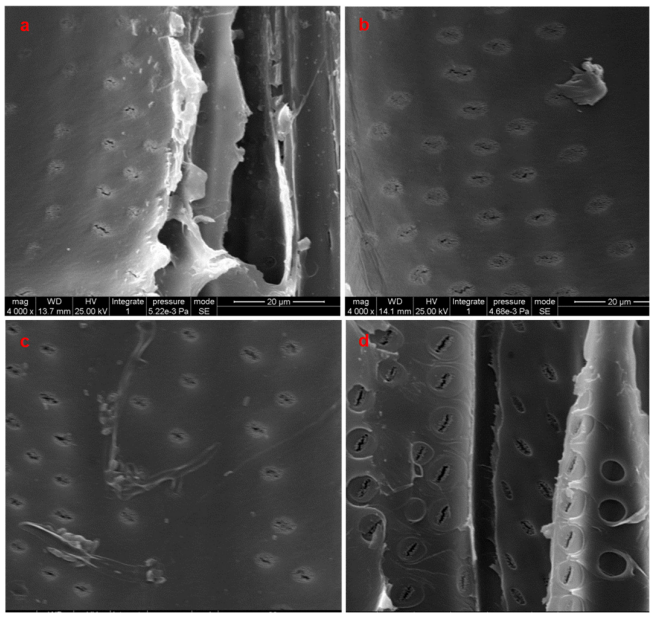

Figure 8. SEM micrographs of wood after conventional drying (**a**: 50 °C/60% RH) and 1 h of SCD at different pressures (**b**: 10 MPa, **c**: 20 MPa, **d**: 30 MPa).

3.6. Permeability of Wood Dried after Supercritical CO_2 Drying

The water absorption ratio of specimens after 1 h of SCD at different pressures is presented in Figure 9. As can be seen, the water absorption rate was fast in the first 6 h, and then it increased

slowly until becoming constant. Moreover, the water absorption rate was obviously different for the specimens after SCD, showing the fastest water absorption rate at 20 MPa and the lowest at 10 MPa. The increased water absorption ratio shows improvement of wood permeability, and this result is in agreement with previous studies [29,32]. The improved permeability of wood is attributed to extracts reduction in wood and micro tissue change of cell walls during SCD. It can be seen that extract yields of wood after SCD was decreased (Figure 7) and bored pit membranes were broken up after SCD (Figure 8). Hold pressure presented the same effect on improvement of drying rate and wood permeability (Figures 4 and 9), and this is because lumen water expulsion efficiency was influenced by wood permeability [37].

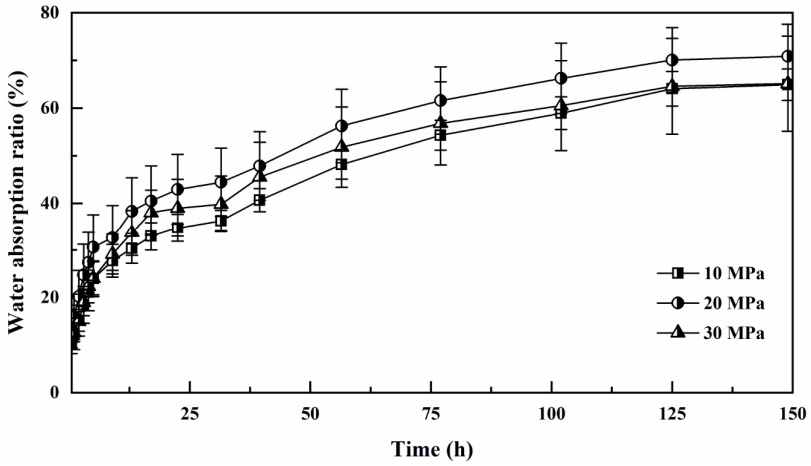

Figure 9. Water absorption ratio of wood after 1 h of SCD at different pressures.

4. Conclusions

The moisture content distribution and transfer property as well as the permeability and extractives of *Eucalyptus urophydis* wood after supercritical CO_2 drying were measured and studied. SCD has a great drying rate, and the drying rate was increased with pressure below 20 MPa, which did not show a positive relation to higher pressure conditions. The pressure played a critical role in water removal from wood, which is the key factor for the drying process and drying schedule building. The moisture contents were higher in the middle of specimens and in the interior of transverse sections of wood. Moisture distributions were more uneven in the condition of low pressure at 10 MPa and in the middle transverse sections of wood. The MC gradient in the tangential direction was greater than in the longitudinal direction, suggesting that water was expelled mostly in the tangential direction of wood. More extractives in the wood were removed by SCD in higher pressure condition. More bordered pits were broken up in the higher pressure SCD. Permeability of wood was improved after SCD due to the reduced extractives and increased amount of opened bordered pits.

Author Contributions: Writing—original draft preparation, L.Y.; writing—review and editing, H.L. and L.Y. All authors have read and agreed to the published version of the manuscript.

Funding: This research was funded by the National Natural Science Foundation of China (Grant No. 31870545 and 31570558) and the Key Laboratory of Bio-based Material Science and Technology (Northeast Forestry University), Ministry of Education (SWZ-MS201903).

Acknowledgments: Special acknowledgment is extended to the Huaan Supercritical Fluid Extraction Co., Ltd. for their assistance.

Conflicts of Interest: The authors declare no conflicts of interest.

References

1. Yang, L.; Mao, H.Z.; Liu, H.H.; Wu, Z.H. Effect of freezing and compressing pre-treatment on collapse of Eucalyptus urophylla E. grandis during drying. *J. For. Eng.* **2018**, *3*, 30–34, doi:10.13360/j.issn.2096-1359.2018.04.005.
2. Ananias, R.A.; Sepulveda-Villarroel, V.; Perez-Pena, N.; Leandro-Zuniga, L.; Salvo-Sepulveda, L.; Salinas-Lira, C.; Cloutier, A.; Elustondo, D.M. Collapse of *Eucalyptus Nitens* Wood after Drying Depending on the Radial Location within the Stem. *Dry. Technol.* **2014**, *32*, 1699–1705, doi:10.1080/07373937.2014.924132.
3. Blakemore, P.; Northway, R. Review of, and Recommendations for, Research into Preventing or Ameliorating Drying Related Internal and Surface Checking in Commercially Important Hardwood Species in South-eastern Australia. In *FWPA Project: PNB047-0809*; FWPA: Federal Way, WA, USA, 2009.
4. Wu, Y.H.; Jia, R.; Ren, H.Q.; Zhou, Y.D.; Xing, X.T.; Wu, Z.K.; Wang, Y.R. Study on radial variation of main physical properties of imported Pinus radiata wood. *J. For. Eng.* **2019**, *4*, 48–53, doi:10.13360/j.issn.2096-1359.2019.06.007.
5. Chafe, S.C. The Distribution and Interrelationship of Collapse, Volumetric Shrinkage, Moisture Content and Density in Trees of *Eucalyptus Regnans* F. Muell. *Wood Sci. Technol.* **1985**, *19*, 329–345, doi:10.1007/BF00350810.
6. Kauman, W.G. Cell Collapse in Wood—Part I: Process Variables and Collapse Recovery. *Holz. Roh. Werkst.* **1964**, *22*, 183–196, doi:10.1007/BF02613024.
7. Kong, L.L.; Zhao, Z.J.; He, Z.B.; Yi, S.L. Development of Schedule to Steaming Prior to Drying and Its Effects on *Eucalyptus grandis* × *E. urophylla* Wood. *Eur. J. Wood Wood Prod.* **2018**, *76*, 591–600, doi:10.1007/s00107-017-1199-2.
8. Peres, M.L.; Delucis, R.D.A.; Gatto, D.A.; Reltrame, R. Solid Wood Bending of Eucalyptus grandis Wood Plasticized by Steam and Boiling. *Ambient. Constr.* **2015**, *15*, 169–177, doi:10.1590/s1678-86212015000200020.
9. Zhang, Y.L.; Miao, P.; Zhuang, S.Z.; Wang, X.M.; Xia, J.W.; Wu, L.M. Improving the Dry-Ability of Eucalyptus by Pre-Microwave or Pre-Freezing Treatment (in Chinese). *J. Nanjing For. Univ.* **2011**, *35*, 61–64.
10. Vermaas, H.F. Drying Eucalypts for Quality: Material Characteristics, Pre-Drying Treatments, Drying Methods, Schedules and Optimization of Drying Quality. *S. Afr. For. J.* **1995**, *174*, 41–49, doi:10.1080/00382167.1995.9629877.
11. Santos, J.A. Recovering Dimension and Form in Collapse Distorted Boards. In Proceedings of the 4th Cost E15 Workshop, Santiago de Compostela, Spain, 30–31 May 2002.
12. Hansmann, C.; Stingl, R.; Prieto, O.G.; Lopez, C.B.; Resch, H. High-Frequency Energy-Asisted Vacuum Drying of Fresh *Eucalyptus globulus*. *Dry. Technol.* **2008**, *26*, 611–616, doi:10.1080/07373930801946759.
13. Yang, L.; Ma, Q.Y.; Liu, H.H.; Liao, X.M.; Wu, Z.H. Freeze-Drying Properties of *Eucalyptus urophylla* × *E. grandis* Wood. *J. For. Environ.* **2018**, *38*, 277–283. (In Chinese)
14. Gabitov, R.F.; Khairutdinov, V.F.; Gumerov, F.M.; Gabitov, F.R.; Zaripov, Z.I.; Gaifullina, R.; Farakhov, M.I. Drying and Impregnation of Wood with Propiconazole Using Supercritical Carbon Dioxide. *Russ J. Phys. Chem. B* **2017**, *11*, 1223–1230, doi:10.1134/S1990793117080048.
15. Cabeza, L.F.; de Gracia, A.; Fernández, A.I.; Farid, M.M. Supercritical CO_2 as Heat Transfer Fluid: A Review. *Appl. Therm. Eng.* **2017**, *125*, 799–810, doi:10.1016/j.applthermaleng.**2017**.07.049.
16. Ramsey, E.; Sun, Q.B.; Zhang, Z.Q.; Zhang, C.M.; Gou, W. Mini-Review: Green sustainable processes using supercritical fluid carbon dioxide. *J. Environ. Sci.* **2009**, *21*, 720–726, doi:10.1016/S1001-0742(08)62330-X.
17. Franich, R.A.; Gallagher, S.; Kroese, H. Dewatering Green Sapwood Using Carbon Dioxide Cycled between Supercritical Fluid and Gas Phase. *J. Supercrit. Fluids* **2014**, *89*, 113–118, doi:10.1016/j.supflu.2014.02.019.
18. 18Dawson, B.S.W.; Pearson, H.; Kroese, H.W.; Sargent, R. Effect of Specimen Dimension and Pre-heating Temperature on Supercritical CO_2 Dewatering of Radiata Pine Sapwood. *Holzforschung* **2015**, *69*, 421–430, doi:10.1515/hf-2014-0055.
19. 19Zuo, C.L.; Cao, Y.J.; Zhou, Y. A Review of Formation Mechanism and Control of Collapse in Eucalyptus Wood. *World For. Res.* **2016**, *29*, 58–63, doi:10.13348/j.cnki.sjlyyj.2016.01.007. (In Chinese)
20. 20Dawson, B.S.W.; Pearson, H. Effect of Supercritical CO_2 Dewatering Followed by Oven-Drying of Softwood and Hardwood Timbers. *Wood Sci. Technol.* **2017**, *51*, 771–784, doi:10.1007/s00226-017-0895-8.
21. Dawson, B.S.W.; Pearson, H.; Kimberley, M.O.; Davy, B.; Dickson, A.R. Effect of Supercritical CO_2 Treatment and Kiln Drying on Collapse in *Eucalyptus nitens* Wood. *Eur. J. Wood Wood Prod.* **2020**, *78*, 209–217, doi:10.1007/s00107-020-01500-5.

22. Li, Z.; Lu, J.X.; Cao, J.Z.; Jiang, J.L. Comparative Study of the Hydrothermal Softening Characteristics of Heartwood and Sapwood. *For. Prod. J.* **2020**, *70*, 243–248, doi:10.13073/FPJ-D-20-00013.
23. Zhang, J.W.; Liu, H.H.; Yang, H.; Yang, L. Drying Characteristics of *Eucalyptus urophylla* × *E. grandis* with Supercritical CO2. *Materials* **2020**, *13*, 3989, doi:10.3390/ma13183989.
24. Behr, V.C.; Hill, S.J.; Meder, R.; Sandquist, D.; Hindmarsh, J.P.; Franich, R.A.; Newman, R.H.Carbon-13 NMR Chemical-shift Imaging Study of Dewatering of Green Sapwood by Cycling Carbon Dioxide between the Supercritical Fluid and Gas Phases. *J. Supercrit. Fluids* **2014**, *95*, 35–540, doi:10.1016/j.supflu.2014.08.026.
25. Newman, R.H.; Franich, R.A.; Meder, R.; Hill, S.J.; Kroese, H.; Sandquist, D.; Hindmarsh, J.; Schmid, M.W.; Fuchs, J.; Behr, V.C. Proton Magnetic Resonance Imaging used to Investigate Dewatering of Green Sapwood by Cycling Carbon Dioxide between Supercritical Fluid and Gas Phase. *J. Supercrit. Fluids* **2016**, *111*, 36–42, doi:10.1016/j.supflu.2016.01.007.
26. Meder, R.; Franich, R.A.; Callaghan, P.T.; Behr, V.C. A Comparative Study of Dewatering of Pinus Radiata Sapwood using Supercritical CO_2 and Conventional Forced Air-drying via in situ Magnetic Resonance Microimaging (MRI). *Holzforschung* **2015**, *69*, 1137–1142, doi:10.1515/hf-2014-0134.
27. Franich, R.A.; Meder, R.; Falge, M.; Fuchs, J.; Behr, V.C. Uncovering Supercritical CO_2 Wood Dewatering via Interleaved 1H-imaging and 13C-spectroscopy with Real-time Reconstruction. *J. Supercrit. Fluids* **2019**, *144*, 56–62, doi:10.1016/j.supflu.**2018**.10.006.
28. 28Ehsan, M.M.; Guan, Z.Q.; Klimenko, A.Y. A Comprehensive Review on Heat Transfer and Pressure Drop Characteristics and Correlations with Supercritical CO_2 under Heating and Cooling Applications. *Renew. Sustain. Energy Rev*. **2018**, *92*, 658–675, doi:10.1016/j.rser.2018.04.106.
29. Jiang, T.; Zhou, Z.F.; Wang, Q.B. Effects of Intensive Microwave Irradiation on the Permeability of Larch Wood. *Scientia Silvae Sinicae* **2006**, *42*, 87–92, doi:10.11707/j.1001-7488.20061116.
30. Fernandes, J.; Kjellow, A.W.; Henriksen, O. Modeling and Optimization of the Supercritical Wood Impregnation Process-Focus on Pressure and Temperature. *J. Supercrit. Fluids* **2012**, *66*, 307–314, doi:10.1016/j.supflu.2012.03.003.
31. Hou, S.X.; Maitland, G.C.; Trusler, M. Measurement and Modeling of the Phase Behavior of the (Carbon Dioxide + Water) Mixture at Temperatures from 298.15K to 448.15K. *J. Supercrit. Fluids* **2013**, *73*, 87–96, doi:10.1016/j.supflu.2012.11.011.
32. Phillips, E.W.J. Identification of Softwoods by Their Microscopic Structure. In *Forest Products Research Bulletin No.22*; DSIR: London, UK, 1948; Volume 22, pp. 1–56.
33. Way, D.; Kamke, F.A.; Sinha, A. Moisture Transport in Wood-Based Structural Panels under Transient Hygroscopic Conditions. *For. Prod. J*. **2020**, *70*, 283–292, doi:10.13073/FPJ-D-20-00012.
34. Peng, W.X.; Wu, X.B.; Wu, Y.Q.; Chen, H. Analysis of Benzene/Ethanol Extractives from Flesh and Old *Eucalyptus urophydis* Chips by Py-GC/MS. *JSCUT* **2009**, *37*, 67–74.
35. Cornelio-Santiago, H.P.; Gonçalves, C.B.; de Oliveira, N.A.; de Oliveira, A.L. Supercritical CO_2 Extraction of Oil from Green Coffee Beans: Solubility, Triacylglycerol Composition, Thermophysical Properties and Thermodynamic Modelling. *J. Supercrit. Fluids* **2017**, *128*, 386–394, doi:10.1016/j.supflu.2017.05.030.
36. Kjellow, A.W.; Henriksen, O. Supercritical Wood Impregnation. *J. Supercrit. Fluids* **2009**, *50*, 297–304, doi:10.1016/j.supflu.2009.06.013.
37. Pearson, H.; Dawson, B.; Kimberley, M.; Davy, B. Predictive Modelling of Supercritical CO_2 Dewatering of Capillary Tubes. *J. Supercrit. Fluids* **2019**, *143*, 198–204, doi:10.1016/j.supflu.2018.08.016.